

A New Vegetation Index Based on the  
Universal Pattern Decomposition Method

L.F.Zhang, S.Furumi, K.Muramatsu, N.Fujiwara,  
M.Daigo and L.P.Zhang

2004.9.15

# A New Vegetation Index Based on the Universal Pattern Decomposition Method

L.F. Zhang<sup>1</sup>, S. Furumi<sup>2</sup>, K. Murumatsu<sup>2,4</sup>, N. Fujiwara<sup>2</sup>, M. Daigo<sup>3</sup> and L.P. Zhang<sup>1</sup>

<sup>1</sup> National Key Laboratory for Information Engineering in Surveying, Mapping and Remote Sensing, Wuhan University, 129 Luoyu Road, Wuhan 430079, P. R. China

<sup>2</sup> Laboratory of Nature Information Science, Department of Information and Computer Sciences, Nara Women's University, Nara, Japan

<sup>3</sup> Department of Economics, Doshisha University, Kyoto, Japan

<sup>4</sup> KYOUSEI Science Center for Life and Nature, Nara Women's University, Nara, Japan

**Abstract.** This study examined a new vegetation index, based on the universal pattern decomposition method (VIUPD). The universal pattern decomposition method (UPDM) allows for sensor-independent spectral analysis. Each pixel is expressed as the linear sum of standard spectral patterns for water, vegetation, and soil, with supplementary patterns included when necessary. Pattern decomposition coefficients for each pixel contain almost all the sensor-derived information, while having the benefit of sensor independence. The VIUPD is expressed as a linear sum of the pattern decomposition coefficients; thus, the VIUPD is a sensor-independent index. Here, the VIUPD was used to examine vegetation amounts and degree of terrestrial vegetation vigor; VIUPD results were compared with results by the normalized difference vegetation index (NDVI), an enhanced vegetation index (EVI), and a conventional vegetation index based on pattern decomposition (VIPD). The results showed that the VIUPD reflects vegetation and vegetation activity more sensitively than the NDVI and EVI.

## 1. Introduction

Researchers have used vegetation indices (VIs) to quantify green-leaf vegetation and to monitor major vegetation fluctuations and associated environmental effects. Studies involving land-cover classifications, environmental monitoring, and deforestation, desertification, or drought brought on by climate change, have employed vegetation indices. Various vegetation indices have been developed for specific research objectives.

Vegetation indices (VI) are spectral transformations of two or more bands designed to enhance vegetation properties and allow for reliable representations of photosynthetic activity and structural canopy variations (Huete *et al.*, 2002). A commonly used index is the normalized difference vegetation index (NDVI), given as follows:

$$NDVI = \frac{\rho_{NIR} - \rho_{red}}{\rho_{NIR} + \rho_{red}}. \quad (1)$$

The NDVI is an important component of local, regional, and global vegetation change studies; however, it uses only red and near infrared reflectance data (Nemani *et al.*, 1993). The enhanced vegetation index (EVI) uses the red and near infrared bands, and also includes blue-band reflectance data to correct for aerosol influences in the red band, and some other aerosol resistance

coefficients (Huete *et al.*, 2002). The EVI is given as follows:

$$EVI = G \frac{\rho_{NIR} - \rho_{red}}{\rho_{NIR} + C_1 \times \rho_{red} - C_2 \times \rho_{blue} + L}, \quad (2)$$

where  $\rho$  values are atmospherically corrected or partially atmospherically corrected (e.g., for Rayleigh and ozone absorption) surface reflectances;  $L$  is the canopy with background adjustment addressing nonlinear, differential near infrared- and red-band radiant transfer through the canopy; and  $C_1, C_2$  are aerosol resistance coefficients that use the blue band to correct for red-band aerosol influences. The coefficients of the EVI algorithm are  $L = 1$ ,  $C_1 = 6$ ,  $C_2 = 7.5$ , and  $G = 2.5$ , where  $G$  is the gain factor (Huete *et al.*, 1994, 1997).

The above methods use either two or three satellite-observed wavelength bands, or require some additional coefficient inputs. We developed a new vegetation index based on the pattern decomposition method (VIPD; Hayashi *et al.*, 1998). The pattern decomposition method (PDM) is a type of spectral mixing analysis (Adams *et al.*, 1995) in which each pixel is expressed as the linear sum of fixed standard spectral patterns for water, vegetation, and soil:

$$VIPD = \frac{\{C_v - C_s - (\frac{S_s}{\sum_{i=1}^n A_i})C_w + S_s\}}{(S_v + S_s)}, \quad (3)$$

where  $C_w, C_v, C_s$  are coefficients for water, vegetation, and soil, respectively;  $S_v, S_s$  represent the total reduced albedo value of vegetation and soil, respectively; and  $A_i$  refers to the reduced albedo value of band  $i$ .

Our analyses showed that the VIPD is more sensitive than the NDVI for determining the vegetation cover ratio, vertical vegetation thickness, and vegetation type (e.g., broad leaf or needle leaf) when using Global Imager (GLI) data. However, since the PDM has sensor-dependent parameters, and the constant values of  $S_v$  and  $S_s$  are sensor-dependent, it is difficult to directly compare results obtained using data from different sensors.

Thus, we developed a sensor-independent universal pattern decomposition method (UPDM) for hyper-multi-spectral data analysis (Zhang *et al.*, 2004). Analysis results demonstrated that the four coefficients (i.e., three standard pattern decomposition coefficients and a supplementary coefficient) calculated by the universal pattern decomposition method are sensor independent. We have now developed a new vegetation index that is based on the universal pattern decomposition method, which we call the VIUPD, and we publish it here for the first time. This vegetation index based on the UPDM has many benefits over the conventional VIPD. The VIUPD is defined as a linear sum of the pattern decomposition coefficients but is sensor independent. In this paper, we compare how our new vegetation index (VIUPD), the NDVI, the EVI, and the VIPD represent the relationships between photosynthesis, the vegetation area ratio, and the number of overlapping leaves.

## 2. A vegetation index (VIUPD) based on the UPDM and multi-spectral data

### 2.1 The universal pattern decomposition method (UPDM)

We developed a universal pattern decomposition method (Zhang *et al.*, 2004) in which reflectance (or brightness) data for each pixel observed by a sensor are decomposed into standard spectral patterns of water, vegetation, and soil as follows:

$$R(i) \rightarrow C_w \cdot P_w(i) + C_v \cdot P_v(i) + C_s \cdot P_s(i), \quad (4)$$

where  $R(i)$  is the reflectance of band  $i$  measured on the ground (or by satellite sensor) for any sample (or any pixel), and  $C_w$ ,  $C_v$ , and  $C_s$  are the decomposition coefficients.

For some studies, a UPDM with only three components is adequate. However, other studies may require more detailed analysis of vegetation change. Thus, we added a yellow-leaf coefficient as a supplementary spectral pattern, changing Equation (4) to

$$R(i) \rightarrow C_w \cdot P_w(i) + C_v \cdot P_v(i) + C_s \cdot P_s(i) + C_4 \cdot P_4(i), \quad (5)$$

where  $C_4$  represents the supplementary pattern coefficients of a yellow leaf, and  $P_w(i)$ ,  $P_v(i)$ ,  $P_s(i)$ , and  $P_4(i)$  are the standard spectral patterns of water, vegetation, soil, and the supplementary yellow-leaf pattern for band  $i$  ( $i$  represents the sensor band numbers), intercepted from  $P_k(\lambda)$  ( $k=w, v, s, 4$ ) as follows:

$$P_k(\lambda) = \frac{\int d\lambda}{\int |R_k(\lambda)| d\lambda} R_k(\lambda), \quad (6)$$

where  $R_k(\lambda)$  values are the spectral reflectance patterns of standard objects. The shapes and magnitudes of the standard patterns  $P_k(\lambda)$  are fixed for any sensor. The  $P_4(\lambda)$  value is defined using the yellow-leaf residual and the three components as follows:

$$P_4(\lambda) = \frac{r_4(\lambda) \int d\lambda}{\int |r_4(\lambda)| d\lambda}, \quad (7)$$

where  $r_4(\lambda)$  is the residual value for a yellow leaf for the  $i$  band,

$$r_4(\lambda) = R_4(\lambda) - \{C_w P_w(\lambda) + C_v P_v(\lambda) + C_s P_s(\lambda)\}, \quad (8)$$

$R_4(\lambda)$  is the measured value of the sample yellow leaf, and  $r_4(\lambda)$  is the residual value. The standard patterns are normalized as follows:

$$\int |P_k(\lambda)| d\lambda = \int d\lambda \quad (k = w, v, s, 4). \quad (9)$$

We intercepted  $P_k(\lambda)$  values for each sensor. The four standard patterns for each sensor are defined by

$$P_k(i) = \frac{\int_{\lambda_{si}}^{\lambda_{ei}} P_k(\lambda) d\lambda}{\int_{\lambda_{si}}^{\lambda_{ei}} d\lambda} \quad (k = w, v, s, 4), \quad (10)$$

where  $\lambda_{si}$  and  $\lambda_{ei}$  are the start and end wavelengths of sensor band  $i$ , respectively, and  $\int_{\lambda_{si}}^{\lambda_{ei}} d\lambda$  is the wavelength width of

band  $i$ .

## 2.2 Vegetation index VIUPD for multi-spectral data

Vegetation indices play an important role in monitoring global surface vegetation change. Ideally, a vegetation index should reflect the amount of vegetation and the degree of vegetation vigor. The amount of vegetation can be expressed by the biomass or leaf area index (LAI). A vegetation index based on pattern decomposition (VIPD) expresses the linear sum of the three pattern decomposition coefficients (Hayashi *et al.*, 1998) and is linear to the vegetation cover ratio (Furumi *et al.*, 1998). However, the VIPD has sensor-dependent parameters. We thus developed a new vegetation index that was based on four pattern decomposition coefficients (i.e., a supplemental spectral pattern plus the three standard patterns) (Daigo *et al.*, 2004). The new vegetation index (or revised VIPD) was normalized by total reflectance or total brightness to minimize shadow effects and obtain stable values. However, the index still used conventional pattern decomposition coefficients.

We have now redefined the vegetation index by producing a vegetation index that is based on a universal pattern decomposition method (VIUPD). The index is a function of the linear combination of the pattern decomposition coefficients. The formula is given as follows:

$$VIUPD = \frac{(C_v - a \times C_s - C_4)}{C_w + C_v + C_s}, \quad (11)$$

where  $(C_w + C_v + C_s)$  represents the sum of total reflectance, and  $a$  is the coefficient of standard soil pattern coefficients. The  $C_s$  term in the numerator is a correction term for dead vegetation, because the spectral pattern for dead vegetation contains a small portion of the vegetation pattern. We determined parameter  $a$  so that the average VIUPD value for dead vegetation equals zero. For standard vegetation, the VIUPD value equals 1.

As mentioned above, a vegetation index should be sensitive to photosynthesis. Plants transform sunlight to chemical energy by photosynthesis. During this process, plants fix carbon dioxide and release oxygen while coping with water loss. Photosynthesis measurements are necessary to understand productivity (biomass accumulation) at leaf, plant, or community levels, as well as vegetative responses to environmental stresses. Satellite remote sensors can quantify the fraction of photosynthetically active radiation (PAR) absorbed by vegetation. Research has found that net photosynthesis directly relates to the amount of PAR absorbed by plants. In short, the more visible sunlight a plant absorbs (during the growing season), the more the plant photosynthesizes, and the more productive the plant is. Therefore, as a leaf turns from green to brown (i.e., as the leaf dies) photosynthesis decreases until finally reaching zero. In response,  $\text{CO}_2$  absorption also decreases to zero.

## 3. Data used in this study

### 3.1. Reflectance data

Sample reflectance data used in this analysis were measured outdoors under solar light or indoors under a halogen lamp with a Field Spec FR (Analytical Spectral Devices, Inc.) or MSR7000 (Opto Research Corp.) radio-spectrometer. Both radio-spectrometers give raw spectral values every 1 nm for wavelengths of 350 to 2500 nm. Spectral resolution ranges from 3 to 10 nm with a 1-degree field of view. After measuring spectra for each sample and for a standard white board, reflectance was calculated from the raw spectral digital values of each sample divided by those of the standard white board. We measured about

600 samples, including leaves, soil, water, concrete, and a sandy beach.

### 3.2. Photosynthesis data

We used a LI-6400 photosynthesis open system to measure light photosynthesis. In this system, an air stream with a known CO<sub>2</sub> concentration is constantly passed through the leaf chamber. The air exiting the chamber will have a lower CO<sub>2</sub> concentration than the air entering the chamber. We recorded changes in CO<sub>2</sub> values and the photosynthetic active radiation (PAR) using an LED light sensor. The carbon dioxide concentration in the chamber was about 350 ppm to match the surrounding air, and the air temperature in the chamber was about 28 degrees Centigrade (Furumi *et al.*, 2004). Figure 3.1 shows three typical results for absorbed CO<sub>2</sub> and reflectance for a green leaf (No. 1), yellow leaf (No. 2), and yellow-green leaf (No. 3) of *Ginkgo biloba* tree.

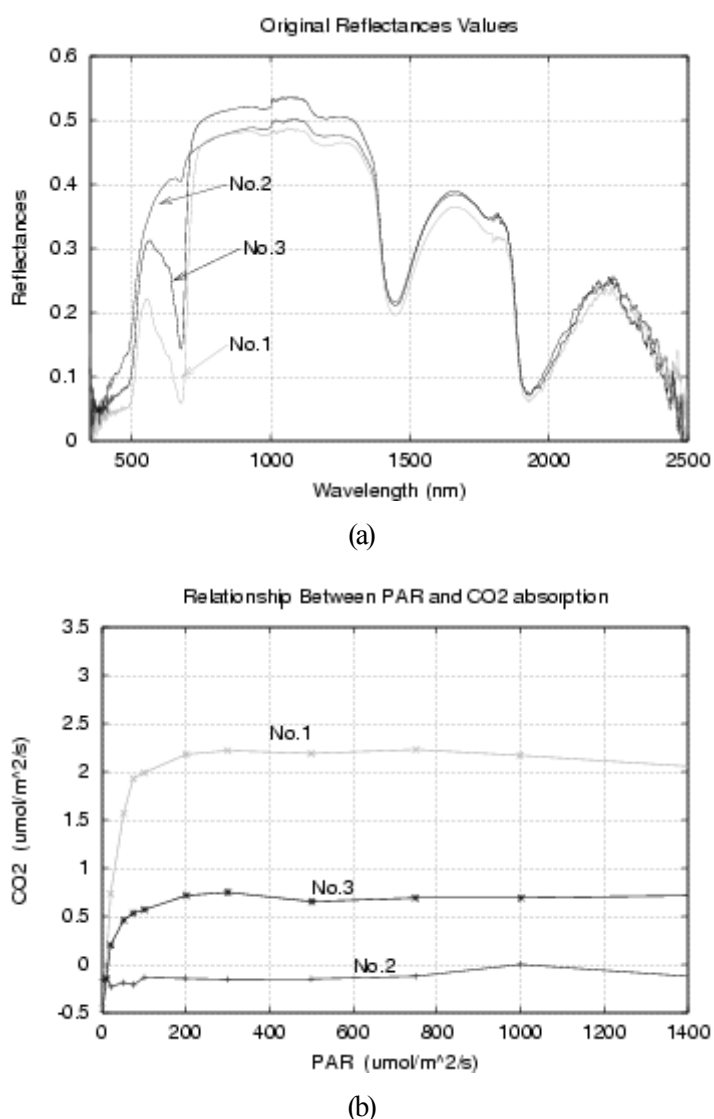


Figure 3.1. Original reflectance patterns of three typical leaves (a), and the relationship between PAR and CO<sub>2</sub> absorption (b)

Table 3.1 lists the photosynthesis data used in this study. In this table, the sample leaves that we measured included *Ginkgo biloba* leaves and *Magnolia praecocissima* leaves, the CO<sub>2</sub> absorption values are correspond to  $P_{max}$ , which is fitted by the least

square regression using the original measured data; the equation is as follows:

$$P(PAR) = \frac{P_{\max} \cdot b \cdot PAR}{1 + b \cdot PAR}, \quad (12)$$

where  $PAR$  represents the photosynthetic active radiation, and  $P_{\max}$  is the maximum photosynthesis in a saturated region,  $b$  refers to the parameter that controls the degree of the fitted curve. When  $PAR$  tends to  $\infty$ , the  $CO_2$  absorption values are approximately equal to  $P_{\max}$ .

Table 3.1 Sample leaves for photosynthesis

Sample number	Sample attribute	$CO_2$ absorption $\mu\text{mol}/(\text{m}^2\cdot\text{s})$	Sample number	Sample attribute	$CO_2$ absorption $\mu\text{mol}/(\text{m}^2\cdot\text{s})$
532	Green leaf	2.05	552	Green leaf	1.62
534	Yellow leaf	-0.17	553	Green leaf	12.58
536	Yellow green	1.30	554	Green leaf	14.59
538	Green leaf	3.56	555	Green leaf	12.60
540	Yellow green	0.82	556	Green leaf	10.47
542	Yellow leaf	-0.22	557	Green leaf	7.69
544	Yellow leaf	-0.28	558	Green leaf	10.78
546	Green leaf	6.10	596	Green leaf	10.62
548	Green leaf	4.69	598	Green leaf	10.45
550	Yellow leaf	1.31			

### 3.2. Other data

To verify the relationship between the VIs and the actual vegetation situation and activity, we measured reflectance,  $CO_2$  absorption, and some other data, such as vegetation land cover ratios and the number of overlapping leaves. For the vegetation area cover ratio, the leaves that we used were obtained from *Cinnamomum camphora* trees, and the soil was collected from the grounds of Nara Women's University of Japan and dried. We measured the reflectance values with changes in the vegetation area cover ratio from 0% to 100%. In addition, we recorded the reflectance of overlapping leaves obtained from *Cinnamomum camphora* trees using 1 to 10 overlapping leaves.

## 4. Results and discussion

### 4.1. Determination of VIUPD parameters

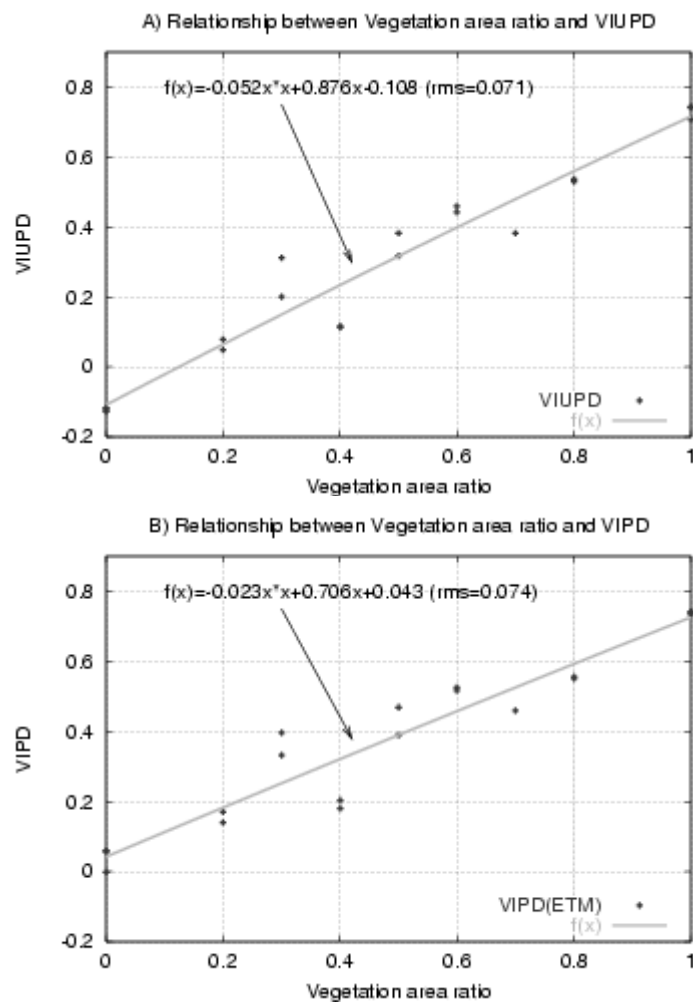
The spectral patterns of dead vegetation resemble soil patterns, but also contain a small amount of the vegetation pattern. Parameter  $a$  in Formula (11) compensates for the vegetation pattern within the dead vegetation pattern. Parameter  $a$  was determined so that the average VIUPD value for 46 samples of ground-measured dead leaves was nearly zero, in this case, the value of  $a$  was 0.10. For this result, Formula (11) is as follows:

$$VIUPD = \frac{(C_v - 0.10 \times C_s - C_4)}{C_w + C_v + C_s}. \quad (13)$$

#### 4.2. Relationship between vegetation indices and the area cover ratio

A number of previous studies have shown that the VIPD is linear to the vegetation cover ratio (e.g., Furumi *et al.*, 1998). Figure 4.1 shows the relationship between various kinds of VI and the vegetation cover ratio for the sample data listed in Table 3.1. In the figure, diagram A shows the relation between EVI and vegetation cover ratio, with the quadratic line fitted by least squares regression using the equation  $f(x) = ax^2 + bx + c$ ; diagrams B, C, and D show relationships for the vegetation cover ratio and NDVI, VIPD, and VIUPD, respectively.

Figure 4.1 shows that the quadratic coefficients of VIPD and VIUPD are smaller than those of EVI and NDVI by one order of magnitude. Thus, VIPD and VIUPD have greater linear correlation with the vegetation cover ratio than EVI and NDVI.



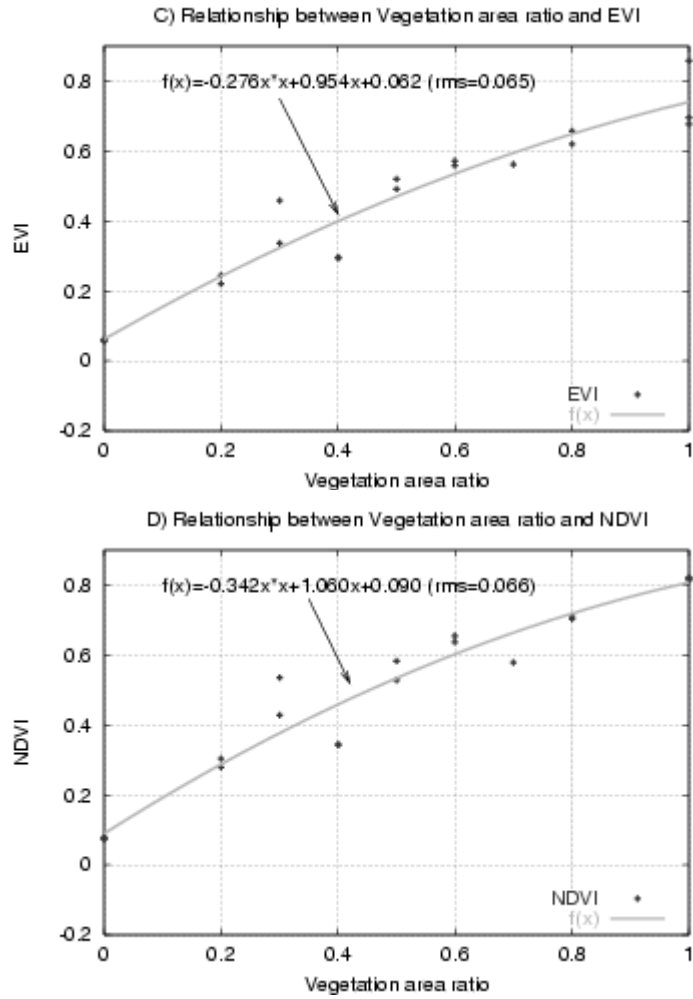
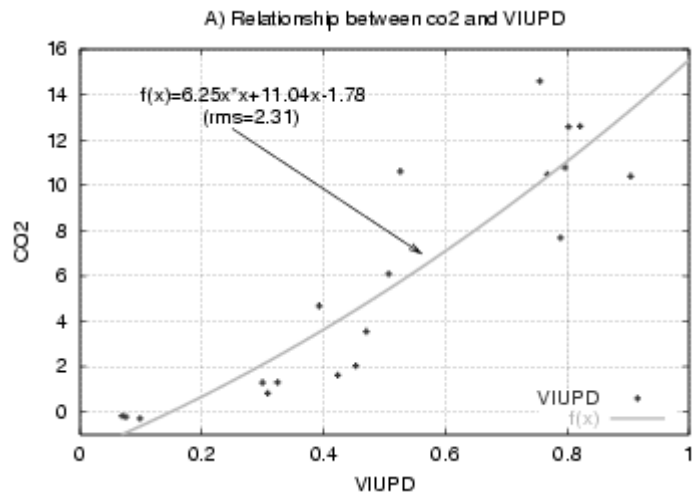


Figure 4.1. Relationships between VIs and the vegetation cover ratio. A) Relationship between the vegetation cover ratio and the VIUPD, B) Relationship between vegetation cover ratio and the VIPD, C) Relationship between vegetation cover ratio and the EVI, D) Relationship between vegetation cover ratio and the NDVI. The solid lines in the figures represent regression results by the equation  $f(x) = ax^2 + bx + c$ .

#### 4.3. Relationship between vegetation indices and gross photosynthetic production



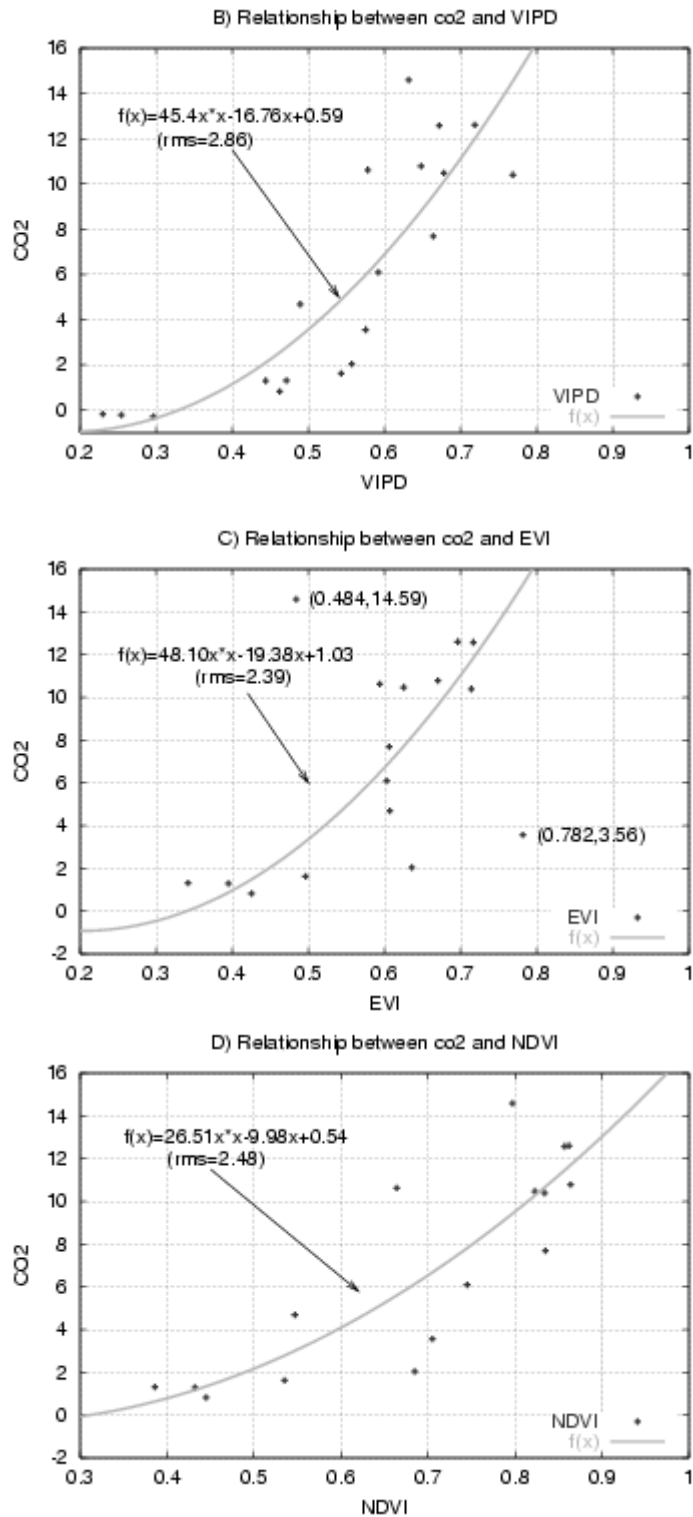


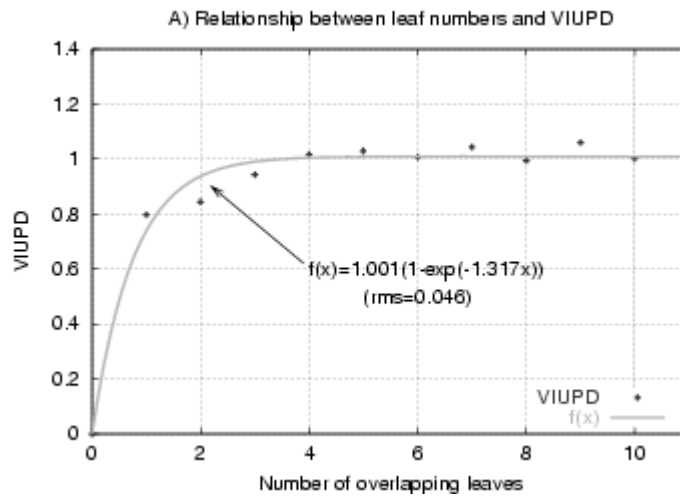
Figure 4.2. Relationships between VIs and gross photosynthetic production. ( $\mu \text{ mol co}_2/\text{m}^2/\text{s}$ ). A) Relationship between  $\text{CO}_2$  absorption and the VIUPD, B) Relationship between  $\text{CO}_2$  absorption and the VIUPD, C) Relationship between  $\text{CO}_2$  absorption and the VIUPD, D) Relationship between  $\text{CO}_2$  absorption and the VIUPD. The solid lines in the figures represent regression results by the equation  $f(x) = ax^2 + bx + c$ .

When sunlight strikes objects, certain wavelengths are absorbed and other wavelengths are reflected. Chlorophyll in plant leaves strongly absorbs visible light (from 0.4 to 0.7 nm) for use in photosynthesis. The leaf cell structure, on the other hand, strongly reflects near-infrared light (from 0.7 to 1.1 nm). The quantity of absorbed CO<sub>2</sub> can reflect vegetation vigor. Plants with higher CO<sub>2</sub> absorption rates can be expected to have greater vegetation index values.

Figure 4.2 shows the relationship between various kinds of vegetation indices and gross photosynthetic production measured on the ground, as described in Section 3. The solid lines in the figures represent regression results by the equation  $f(x) = ax^2 + bx + c$ . The VIUPD showed a much smaller  $a$  coefficient value (6.25) than did the VIPD, EVI, and NDVI. These results suggest that the VIUPD has a greater linear correlation with gross photosynthetic production than do the VIPD, EVI, and NDVI.

#### 4.4. Relationship between vegetation indices and number of overlapping leaves

As described above, the more leaves a plant has, the more light will be reflected as a function of wavelength. A vegetation index should be sensitive to the density or thickness of surface vegetation. In this study, we verified the relation between the number of overlapping leaves and the VIs. Figure 4.3 shows the relationships between the VIs and number of overlapping leaves. The solid lines represent regression results using the formula  $f(x) = a(1 - e^{-bx})$ , the horizontal axes represent the number of overlapping leaves of *Cinnamomum camphora* trees. The results show that the  $b$  coefficient values are smaller for the VIUPD than for the VIPD, EVI, and NDVI. Thus, the VIUPD is more sensitive than the other indices to the number of overlapping leaves.



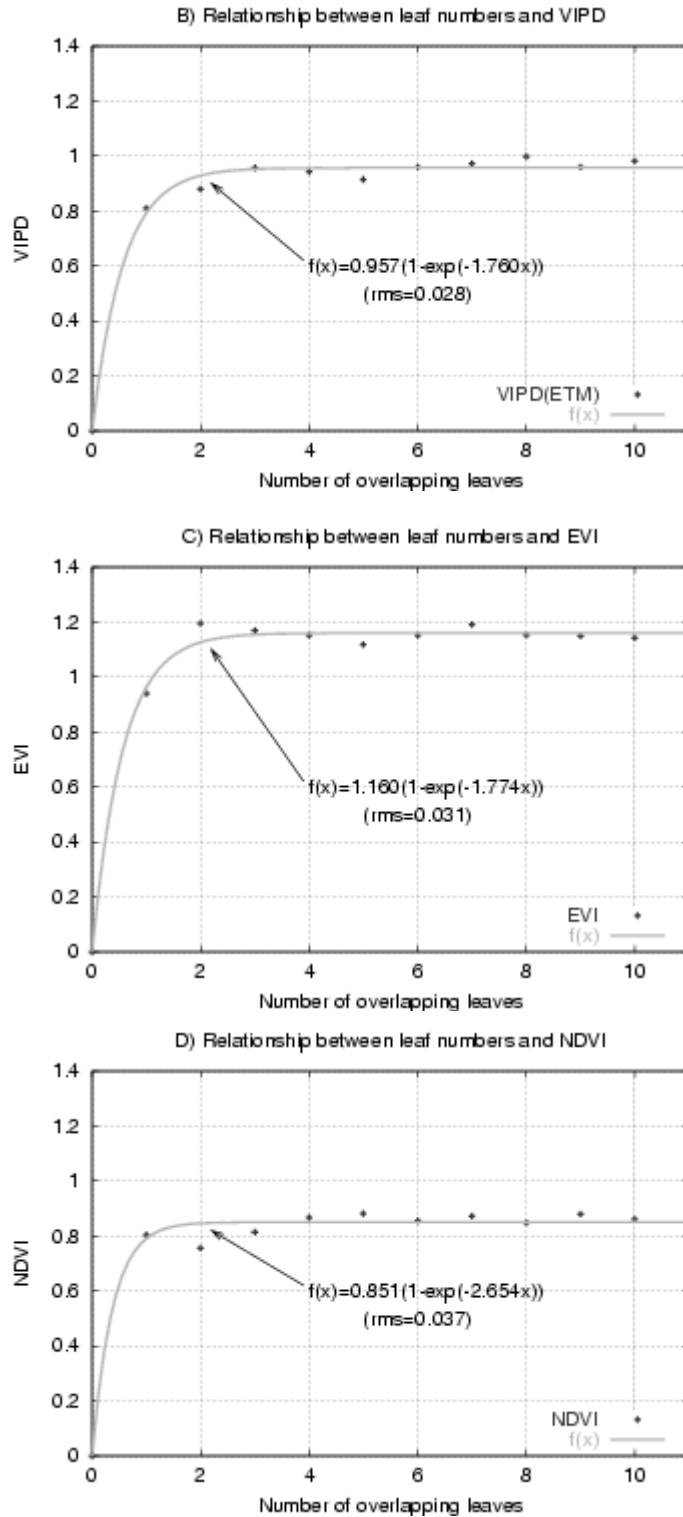


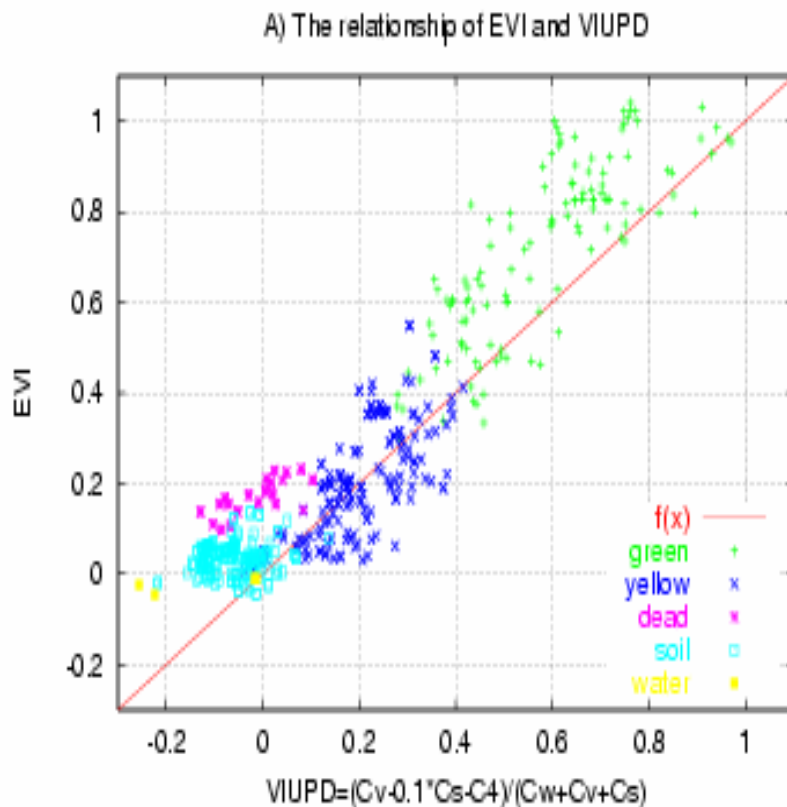
Figure 4.3. Relationships between the VIs and the number of overlapping leaves. A) Relationship between the VIUPD and the number of overlapping leaves, B) Relationship between the VIPD and the number of overlapping leaves. C) Relationship between the EVI and the number of overlapping leaves, D) Relationship between the NDVI and the number of overlapping leaves. The horizontal axes represent the number of overlapping leaves of *Cinnamomum camphora* trees.

#### 4.5. Relationships between vegetation indices

We compared the VIUPD with the EVI, NDVI, and VIPD using various green-leaf, yellow-leaf, dead-leaf, soil, and water samples for a CONTINUE sensor; to calculate the VIs we used the blue (481.0–490.0 nm), red (651.0–660.0nm), and NIR (811.0–820.0 nm) bands. Figure 4.4 illustrates the relationships between selected VIs and the VIUPD. Diagram A shows the relationship between the EVI and VIUPD for about 600 samples; diagram B shows the relationship between the NDVI and VIUPD, and diagram C shows the relationship between the VIPD and VIUPD.

Figure 4.4 demonstrates the sensitivity of all VIs to water, vegetation, and soil. For one part of the yellow-leaf and dead-leaf patterns, the NDVI and EVI show opposite values, that is, some dead-leaf values are bigger than those of yellow-leaves. Since the NDVI and EVI use only two wavelengths (i.e., red and near infrared bands), reflectance corresponding to the two bands is nearly the same for typical yellow leaves, while for typical dead leaves, the reflectance for the red band is smaller than that for the infrared band, as shown in Figure 4.5. Thus, some of the VI values for dead and yellow-leaves shown in Figure 4.4 are reversed. For soil, the VIPD has large positive values, which are compatible with yellow leaves.

Figure 4.4 show that among EVI, NDVI, VIPD, and VIUPD, only VIUPD gives the expected order from green-leaf to water. That is, VIUPD is the best vegetation index among EVI, NDVI, VIPD, and VIUPD.



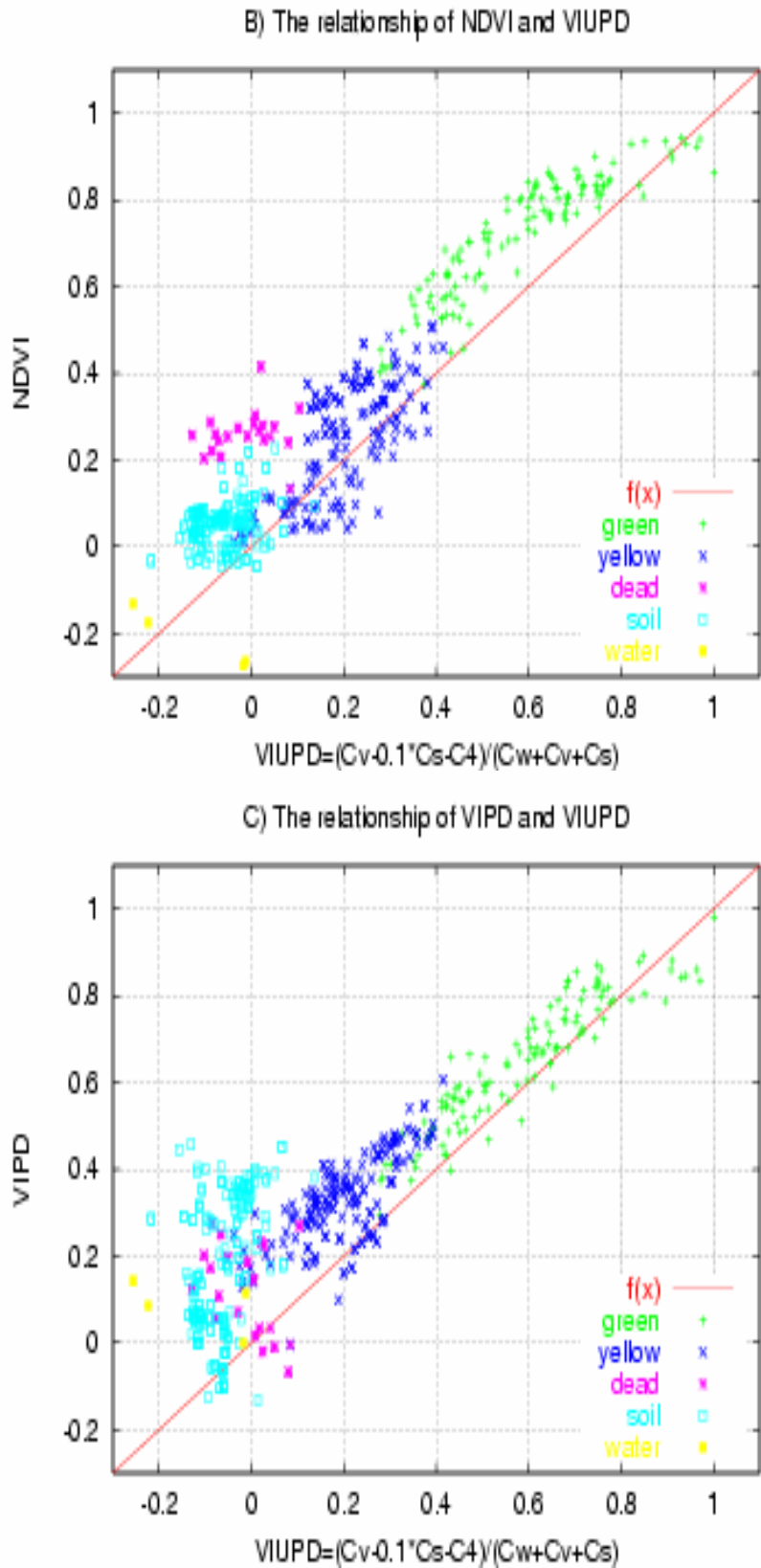


Figure 4.4. Relationships between selected VIs and the VIUPD. A) Relationship between the EVI and the VIUPD, B) Relationship between the NDVI and the VIUPD, C) Relationship between the VIPD and the VIUPD.

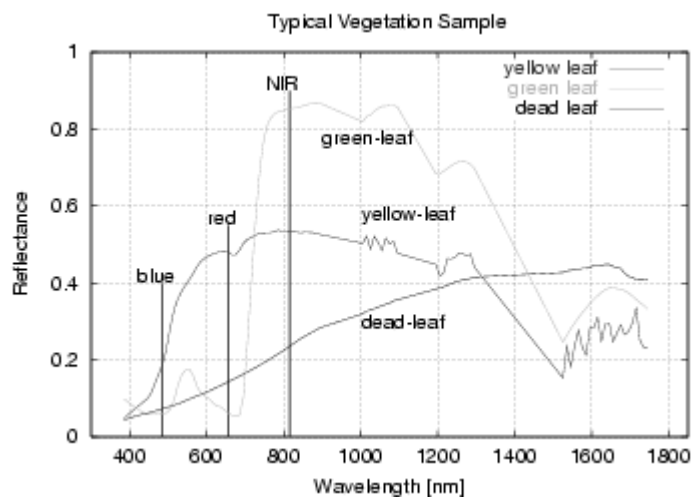


Figure 4.5. Spectral patterns of a typical vegetation sample

## 5. Summary and conclusions

We developed a universal pattern decomposition method to obtain sensor-independent pattern decomposition coefficients. In this paper, a new vegetation index, based on the UPDM, was examined. To investigate how well the method measured vegetation change, we ground-measured about 600 samples, including green-leaf, yellow-leaf, dead-leaf, soil, water, and concrete samples. In addition to the three standard spectral patterns, we used a supplemental yellow-leaf spectral pattern to study vegetation change in detail.

The vegetation index, based on the universal pattern decomposition index (VIUPD), reflects the linear sum of the four pattern decomposition coefficients. The VIUPD reflected vegetation concentrations, the amount of CO<sub>2</sub> absorption, and the degree of terrestrial vegetation vigor more sensitively than did the NDVI and EVI, and was especially sensitive to CO<sub>2</sub> absorption. The NDVI and EVI became more rapidly saturated as a function of PAR. Two or three reflectance bands are used to calculate EVI and NDVI, while the VIUPD and VIPD use multi-spectral satellite- and ground-measured reflectance data. As a sensor-independent index, the VIUPD is more suitable for multi-spectral analysis than the EVI, NDVI, and VIPD. Using multi-spectral data, the VIUPD can provide sensor-independent physical values and allow for direct comparisons using data from various sources.

Future VIUPD research will concentrate on applications using MODIS data and ETM data acquired over the Three Gorges region of China, and will compare VIUPD results with EVI and NDVI results.

## Acknowledgments

This work was supported under the ADEOS-II/GLI Project of the Japan Aerospace Exploration Agency (JAXA), the Academic Frontier Promotion Project of the Ministry of Education, Science, Sports, and Culture of Japan, and the 973 Project of the People's Republic of China (Project Number 2003CB415205).

## References

Adams, J. B., Sabol, D. E., Kapos, V., Filho, R. A., Roberts, D. A., Smith, M. O., and Gillespie, A. R. (1995). "Classification of

- multispectral images based on fractions of endmembers: Application to land-cover change in the Brazilian Amazon,” *Remote Sensing of Environment*, 52, 137-154.
- Crist, E. P., Cicone, R. C. (1984). “A physically based transformation of Thematic Mapper data—The TM Tasseled Cap,” *IEEE Transactions on Geoscience and Remote Sensing*, GE-22, 256-263.
- Daigo, M., Ono, A., Fujiwara, N., and Urabe, R. (2004). “Pattern decomposition method for hyper-multi-spectral data analysis,” *International Journal of Remote Sensing*, 25(6), 1153-1166.
- Fujiwara, N., Muramatsu, K., Awa, S., Hazumi, A. and Ochiai, F. (1996). “Pattern expansion method for satellite data analysis,” (in Japanese). *Journal of Remote Sensing Society of Japan*, 17(3), 17-37.
- Furumi, S., Hayashi, A., Murumatsu, K., and Fujiwara, N. (1998). “Relation between vegetation vigor and new vegetation index based on pattern decomposition method,” *Journal of Remote Sensing Society of Japan*, 18(3), 17-34.
- Furumi, S., Xiong, Y., and Fujiwara, N. (2003). “Establishment of an algorithm to estimate canopy photosynthesis by pattern decomposition using multi-spectral data,” *Journal of Remote Sensing Society of Japan*, (submitted).
- Huete, A., Justice, C., and Liu, H. (1994). “Development of vegetation and soil indices for MODIS-EOS,” *Remote Sensing of Environment*, 49, 224-234.
- Huete, A., Liu, H. Q., Batchily, K., and van Leeuwen, W. J. D. (1997). “A comparison of vegetation indices over a global set of TM images for EOS-MODIS,” *Remote Sensing of Environment*, 59, 440-451.
- Huete, A., Didan, K., Miura, T., Rodriguez, E. P., Gao, X., and Ferreira, L. G. (2002). “Overview of the radiometric and biophysical performance of the MODIS vegetation indices,” *Remote Sensing of Environment*, 83, 195-213.
- Hayashi, A., Muramatsu, K., Furumi, S., Shiono, Y., Fujiwara, N., and Daigo, M. (1998). “An algorithm and a new vegetation index for ADEOS-II/GLI data analysis,” *Journal of Remote Sensing Society of Japan*, 18(2), 28-50.
- Muramatsu, K., Furumi, S., Fujiwara, N., Hayashi, A., Daigo, M., and Ochiai, F. (2000). “Pattern decomposition method in the albedo space for Landsat TM and MSS data analysis,” *International Journal of Remote Sensing*, 21(1), 99-119.
- Nemani, R., Pierce, L., Running, S., and Band, L. (1993). “Forest ecosystem processes at the watershed scale: Sensitivity to remotely-sensed leaf area index estimates,” *International Journal of Remote Sensing*, 14, 2519.
- Zhang, L. F., Furumi, S., Murumatsu, K., Fujiwara, N., Daigo, M., and Zhang, L. P. (2004). “Sensor-independent analysis method for hyper-multi spectra based on the pattern decomposition method,” *International Journal of Remote Sensing*, (submitted).